ACS Chemical Neuroscience

Research Article

pubs.acs.org/chemneuro

The Natural Product Betulinic Acid Rapidly Promotes Amyloid-β Fibril Formation at the Expense of Soluble Oligomers

Matthew S. Planchard, Michael A. Samel, Amit Kumar, and Vijayaraghavan Rangachari*

Department of Chemistry and Biochemistry, University of Southern Mississippi, 118 College Drive #5043, Hattiesburg, Mississippi 39406, United States

Supporting Information

ABSTRACT: The biochemical hallmarks of Alzheimer's disease (AD) are the aggregates of amyloid-β (Aβ) peptide that deposit in brains of AD patients as senile plaques. The monomeric Aβ undergoes aggregation in a nucleation-dependent manner to form insoluble fibrils. Emerging evidence suggests that the low-molecular-weight aggregates called "soluble oligomers" are the primary neurotoxic agents as opposed to the fibrils. Needless to say, developing Aβ aggregation inhibitors is imperative for a meaningful progress toward AD therapy. In this report, we have explored the in vitro interactions between a natural product called betulinic acid (BA) and Aβ42 peptide. BA has found its therapeutic use in several human pathologies including cancer, HIV-related AIDS, and nervous system disorders. The results from this study indicate that BA rapidly promotes the formation of Aβ42 fibrils and, in doing so, partly circumvents the formation of potentially neurotoxic soluble oligomers. Furthermore, the promotion of fibrils by BA seems to be specific for the fibril formation "on-pathway", and it fails to interact with aggregates that are formed outside this obligatory pathway. The unique ability of BA to promote fibrils at the expense of oligomers along with its well-known pharmacological properties make BA a potential therapeutic agent for AD.

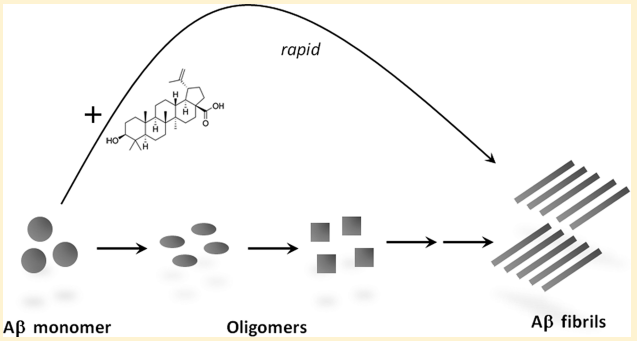

KEYWORDS: *Amyloid, Alzheimer's, betulinic acid, inhibition, drug design and aggregation*

Alzheimer's disease (AD) is the most common among all neurodegenerative diseases and is characterized by acute memory loss and cognitive decline in elderly patients. The pathogenic species responsible for the neuronal loss and toxicity in AD brains is known to be proteinacious aggregates primarily made of a polypeptide called amyloid-β (Aβ) peptide. Aβ is generated extracellularly upon proteolytic processing of amyloid precursor protein (APP), and has a high tendency to aggregate and form amyloid aggregates. The process of aggregation involves the conversion of monomeric Aβ to large, fibrillar, insoluble aggregates that eventually deposit as senile plaques in AD brains. Emerging evidence suggests that, among the various aggregates, low-molecular-weight (LMW) ones, broadly termed as "soluble oligomers" that fall within the range of 2−50mers, are the primary neurotoxic agents responsible for synaptic dysfunction and cognitive decline.[1−4] The Aβ aggregation process is a nucleation-dependent mechanism that follows a sigmoidal growth curve involving a lag phase and a growth phase. In such a process, it is clear that smaller oligomers, which are the intermediates of fibril formation, are transiently formed along the pathway. However, it is also becoming evident from many recent reports that there can be multiple pathways of aggregation,[5−7] and that neurotoxic oligomers can be populated via such alternate pathways that lie outside the obligatory fibril-formation pathway.[8−10]

In the context of drug design, molecules that can interfere with the Aβ aggregation process seem to be an obvious choice, as this process is directly implicated in AD pathology. Indeed, several Aβ aggregation inhibitors have been extensively explored during the past decade. A number of small molecule inhibitors, including some natural products, are reported to disrupt Aβ aggregation in vitro and reduce toxicity.[11−20] Here, we report the interaction of a natural product called betulinic acid (BA) with Aβ42 peptide (one of the two major forms of Aβ peptide) and its effect on the latter's aggregation process. BA is a lupane-type triterpenoid (Figure 1) and is a major component in many different plants including *Bacopa monnieria*, also known as "Bhrami", which largely grows in south Asia.[21] BA has found its therapeutic use both in the ancient Indian form of medicine called "Ayurveda" for the treatment of central nervous system (CNS) disorders, as well as in modern medicine against various carcinomas.[22,23] More

Special Issue: Alzheimer's Disease

Received: March 5, 2012
Accepted: April 16, 2012
Published: April 16, 2012

Aβ42

^{1}DAEFRHDSGY EVHHQKLVFF AEDVGSNKGA IIGLMVGGVV IA^{42}

Aβ42 F19W

^{1}DAEFRHDSGY EVHHQKLV**W**F AEDVGSNKGA IIGLMVGGVV IA^{42}

Betulinic acid (BA)

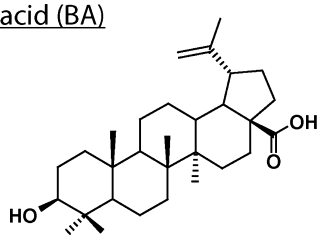

Figure 1. List of compounds used in this study.

importantly, BA is able to cross the blood-brain barrier, which makes it a compound suitable for the treatment of CNS disorders.[21] The well understood pharmacology and the use of BA in the treatment of many disorders encouraged us to explore the potential interactions between BA and Aβ peptide directed toward AD therapy.

In this report, we show that BA binds to Aβ42 and augments its rate of fibril formation in a concentration-dependent manner in vitro. In addition, the augmentation appears to at least partly circumvent the neurotoxic, soluble intermediates along the fibril formation "on-pathway". This unique mechanism of fibril formation that occurs at the expense of neurotoxic oligomers may be useful in developing new therapeutic molecules against AD.

RESULTS

BA Augments Aβ42 Fibril Formation in a Concentration Dependent Manner. The effects of BA on Aβ42

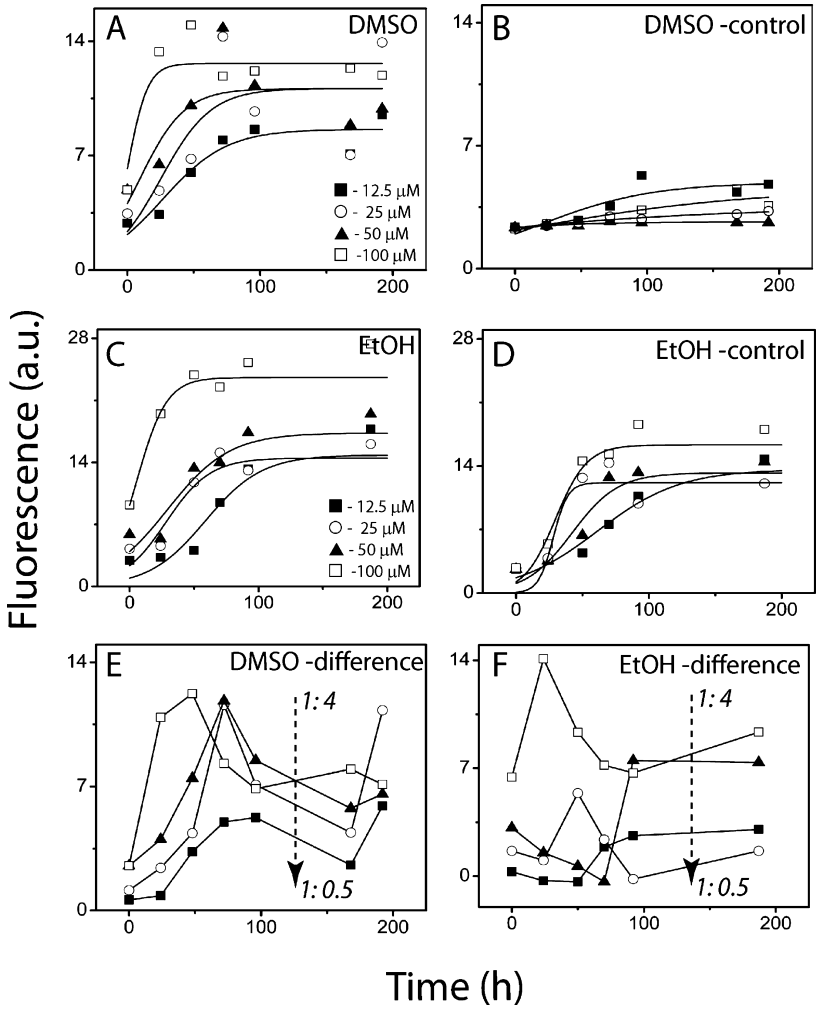

Figure 2. Dose-dependent augmentation of Aβ42 aggregation by BA. Aggregation was measured via ThT fluorescence over time. (A) Incubations composed of 25 μM Aβ42 in 20 mM Tris, pH 8.0 at 37 °C with increasing amounts of BA dissolved in DMSO; 12.5 μM (■), 25 μM (○), 50 μM (▲), 100 μM (□). (B) Controls containing DMSO concentrations corresponding to 12.5, 25, 50, and 100 μM BA incubations, respectively, shown in (A): 0.625% (▲), 1.25% (○), 2.5% (□), and 5% (■). (C) Incubations comprising buffered 25 μM Aβ42 with increasing amounts of BA dissolved in EtOH: 12.5 μM (■), 25 μM (○), 50 μM (▲), and 100 μM (□). (D) Controls containing varing EtOH concentrations: 0.625% (■), 1.25% (○), 2.5% (▲), and 5% (□). (E) Difference plot of BA dissolved in DMSO (A) and DMSO controls (B). The control fluorescence at each time point was subtracted from the fluorescence of the BA samples to generate the plot, which shows the molar stoichiometric incubations, 1:0.5 (■), 1:1 (○), 1:2 (▲), and 1:4 (□). (F) Similar difference plot of BA dissolved in EtOH (C) and EtOH controls (D), which shows the molar stoichiometric incubations, 1:0.5 (■), 1:1 (○), 1:2 (▲), and 1:4 (□). The Aβ:BA stoichiometry is indicated by dotted arrows in (E) and (F).

dx.doi.org/10.1021/cn300030a | ACS Chem. Neurosci. 2012, 3, 900−908

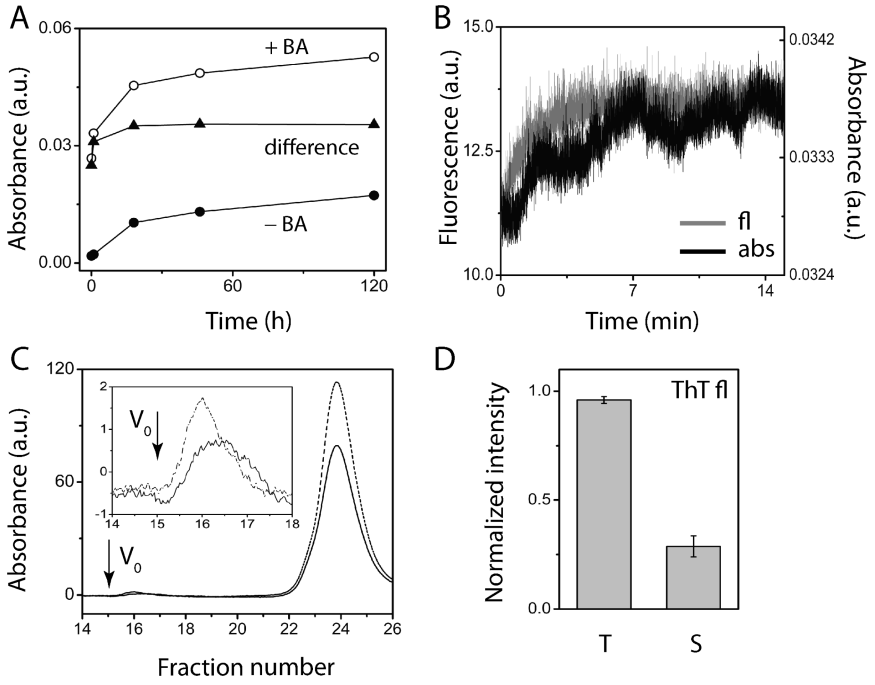

Figure 3. Other assays also suggest rapid Aβ fibrillation induced by BA. (A) Turbidity assay was performed by measuring the absorbance at 400 nm for buffered 25 μM Aβ42 in 5% DMSO at 37 °C in the presence of 100 μM BA (○) or in the absence of BA (●). The difference plot is also shown (▲). (B) Kinetics of the incubations in (A) was monitored immediately after incubation by ThT fluorescence (gray line) or absorbance at 400 nm (black line). (C) Samples in (A) were subjected to fractionation via SEC after 24 h of incubation. The samples were subjected to centrifugation at 19,000*g* for 15 min, and the supernatants were loaded on to the Superdex-75 column. The sample containing BA is shown as a smooth line, whereas the control sample in the absence of BA is shown as a dotted line The monomers eluted at fractions 22−26, while the aggregates peaked near the void volume (V_0) between 15 and 17 (inset). (D) Sedimentation assay was performed by taking an aliquot of the coincubation of Aβ42 with 4-fold molar excess of BA and measuring ThT fluorescence after 24 h (T). In parallel, another aliquot of the same reaction was subjected to centrifugation at 19,000*g* for 15 min. The supernatant thus obtained was measured via ThT fluorescence (S). Three such data sets were averaged.

aggregation were explored by thioflavin-T (ThT) fluorescence. ThT is an extrinsic dye that is known to show fluorescent properties upon binding to amyloid aggregates,[24] and hence, it is used as an indicator to monitor Aβ fibril formation or aggregation. Since BA shows poor solubility in aqueous buffers, all of our experiments were performed in two different solvents: dimethyl sulphoxide (DMSO) and ethanol (EtOH). As described in the subsequent section, EtOH was used as a solvent to facilitate circular dichroism (CD) measurements, as DMSO is not well tolerated in CD. It was therefore essential to monitor aggregation in both solvents in order to ensure the solvent-induced effects were accounted for.

Freshly purified, seed-free monomeric Aβ42 samples (25 μM) were incubated with increasing concentrations of BA (from substoichiometric ratio to 4-fold excess) at 37 °C. Since the stock solutions of BA (1 mM) were prepared in 100% DMSO or EtOH, the incubations of varying Aβ:BA stoichiometry resulted in different final concentrations of DMSO or EtOH in the sample; stoichiometric ratios of 1:4, 1:2, 1:1, and 1:0.5 Aβ42:BA contained 5, 2.5, 1.25, and 0.625%,of DMSO or EtOH, respectively. Therefore, appropriate Aβ42 samples in similar solvents were used as controls. Aliquots of the incubated samples at the given time points were subjected to fluorescence measurement upon addition of ThT buffer as shown in Figure 2A and C for DMSO and EtOH, respectively. The data were fit using a sigmoidal equation (eq 1 in Methods) to obtain lag-time information. Incubation in DMSO showed an increase in Aβ42 aggregation rate as observed by both the increase in the fluorescence intensity and the decrease in lag times as compared to the controls. The difference plots shown in Figure 2E show the dose−response effect in which 1:4 ratio (□) had the highest rate of aggregation, followed by 1:2 (▲), 1:1 (○), and 1:0.5 (■). The 4-fold excess of BA showed an immediate and a sharp increase in ThT fluorescence intensity with no measurable lag-time (□ in Figure 2A and E). Even a substochiometric ratio of 1:0.5 of Aβ42:BA (■ in Figure 2E) resulted in augmentation of the aggregation rate as indicated by the fluorescence increase after ∼50 h of incubation. Similarly, incubations with BA in EtOH also resulted in augmented Aβ42 aggregation rates with lag times similar to those observed with DMSO (Figure 2C). The control incubations in EtOH but in the absence of BA also resulted in increase in Aβ42 aggregation rates. However, the difference plots of the incubations in EtOH showed a net increase in the aggregation rates, which was most prominent with 1:4 stoichiometry of Aβ-to-BA (Figure 2F). It is noteworthy that the incubation at a 1:4 molar ratio showed a rapid increase in ThT fluorescence in both solvents within the first 24 h (Figures 2E and F). Reproducible results were obtained multiple times for both solvents. Although we purify Aβ peptides through size exclusion chromatorgraphy (SEC) to get rid of the preformed aggregates (described in Methods), slight variations in Aβ monomer purity remain due to the presence of small amounts of aggregates that remain unfractionated by SEC. This manifests as differences in the lag times, making it difficult to average the data sets, and thus, we have reported only an individual data set. Nevertheless, in all our experimental sets, the overall reaction profiles with respect to BA concentrations remained nearly identical to the one shown in Figure 2.

dx.doi.org/10.1021/cn300030a | *ACS Chem. Neurosci.* 2012, 3, 900−908

Turbidity, SEC, and Sedimentation Assays Also Indicate Rapid Aβ42 Fibril Formation in the Presence of BA. In order to ensure that the increase in ThT fluorescence observed was indeed due to fibril formation, the aggregation process was monitored by turbidity and sedimentation assays along with fractionation by SEC. Since the maximal effect on Aβ aggregation was observed (in ThT measurements) with a 4-fold molar excess, only samples of 25 μM Aβ42 incubated with 100 μM BA in DMSO were explored in these experiments. First, we monitored aggregation using the turbidity assay, measuring the intensity of light at 400 nm in a UV−vis spectrophotometer as previously described.[25] Aβ42 incubated with BA showed a rapid increase in turbidity within 24 h of incubation, which remained high for the rest of the incubation time, consistent with the ThT experiments (○; Figure 3A). The control Aβ42 sample in the absence of BA also displayed a similar behavior; however, the intensity was much lower than that with BA (●; Figure 3A). The difference curve clearly showed a rapid increase during the initial 24 h that remained fairly stable over remainder of the incubation period (▲; Figure 3A), which was similar to the change observed in the ThT fluorescence experiment (Figure 2A). In order to rule out any experimental aberration that could have led to the sharp increase in fluorescence and absorbance levels, the kinetics of aggregation was monitored immediately upon coincubation of BA and Aβ42 (0 h; Figures 2A and 3A, respectively). As shown in Figure 3B, both ThT fluorescence and absorbance showed a nearly identical exponential increase in respective intensities, suggesting a rapid augmentation of aggregation induced by BA.

In order to quantify the rapid aggregation induced by BA, the depletion of monomers was monitored using a Superdex-75 SEC column. A sample containing 25 μM Aβ42 and 100 μM BA incubated at 37 °C for 24 h was fractionated along with a control without BA incubated in similar conditions. Prior to fractionation, the samples were centrifuged at 19,000*g* for 15 min in order to sediment any insoluble fibrils that may be present, which could obscure sample elution and, consequently, the data, on an SEC column. Only the supernatant was then loaded on to the column for fractionation. The Aβ42 control incubation in the absence of BA showed a distribution containing predominantly a monomeric peak, which eluted in fractions 24 and 25 along with a minor amount of aggregated material eluting near the void volume (V_0) of the column (Figure 3C; dotted line). The Aβ42 sample in the presence of BA showed a similar fractionation profile (Figure 3C; solid line); however, the amount of monomer was less than that of the control sample. This suggests that the presence of BA promotes rapid fibril formation, leading to a concomitant decrease in the amount of monomers. It is interesting to note that the sample with BA also contained some aggregates that eluted near the void volume (Figure 3C; inset). However, the intensity of the aggregate peak was less than that observed for the control sample. Since these aggregates were nonfibrillar soluble intermediates (as the fibrils were sedimented prior to fractionation), this observation suggests that fewer soluble oligomers are generated in the presence of BA. In other words, it suggests that BA promotes insoluble fibril formation at the expense of soluble aggregates.

Finally, in order to ensure that the aggregates formed in the presence of BA were indeed fibrils, a sedimentation assay was performed. After 24 h, a sample containing buffered 25 μM Aβ42 co-incubated with 4-fold excess BA was measured by ThT fluorescence as previously described. The sample was then centrifuged at 19,000*g* for 15 min, and the ThT fluorescence of the supernatant was measured. As shown in Figure 3D (gray bars), only ∼30% of fluorescence was observed after sedimentation, suggesting a large amount of fibril formation within 24 h of incubation. Furthermore, mass spectrometry analyses of supernatant and pellet from the coincubated sample revealed that all BA was associated with the fibrils and none was observed in the supernatant (data not shown). Collectively, the data suggest that BA is able to rapidly promote the formation of insoluble Aβ42 fibrils from monomers and does so possibly by one or both of the following mechanisms: (i) by circumventing the formation of some of the soluble oligomeric intermediates and (ii) by simple kinetic acceleration of the rate of fibril formation. Nevertheless, regardless of the mechanism, BA seems to decrease the steady state concentration of soluble oligomers in the solution.

Oligomers are Absent in Co-incubations of Aβ42 with BA. The samples incubated in Figure 2A and B were also subjected to electrophoresis and immunoblotting to see whether the results complemented the experiments described above. Shown in Figure 4 are immunoblots of samples of Aβ42 with a 4-fold excess of BA prepared in the same manner as those in Figure 2A, along with appropriate controls. Clearly, the control sample in the absence of BA showed no high molecular weight bands for 24 h (Figure 4A: 24 h). After 48 h, aggregate bands of ∼100 kDa were apparent, which were presumably oligomeric intermediates, along with some high molecular weight bands that failed to enter the gel consistent with fibrils (F) (Figure 4A: 48 h). In contrast, samples with BA showed a fibril band (F) within 24 h of incubation. More importantly, the supernatant after centrifuging the sample at 19,000*g* for 15 min failed to show the high molecular weight band (Figure 4B; 24 h, S), confirming that this band corresponded to fibrils. A similar pattern was observed after 48 h of incubation (Figure 4B; 48 h). Although the control sample showed similar bands at 48 h, they were also present in the supernatant, suggesting that the bands may correspond to nonfibrillar, "nonpelletable" forms of

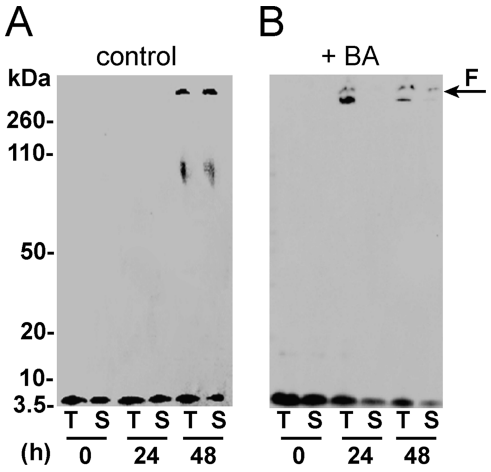

Figure 4. Aβ42 aggregation in the presence of BA monitored by immunoblots. Samples containing 25 μM Aβ42 were incubated alone (control) or with 100 μM BA (+BA) at 37 °C. Aliquots of the sample were taken at the indicated time points and were run on an SDS-PAGE gel followed by Western blotting and immunodetection. The lanes T and S represent total and supernatant (after spinning the sample at 19,000*g* for 15 min to remove fibrils) respectively, after 0, 24, and 48 h of incubation.

dx.doi.org/10.1021/cn300030a | ACS Chem. Neurosci. 2012, 3, 900−908

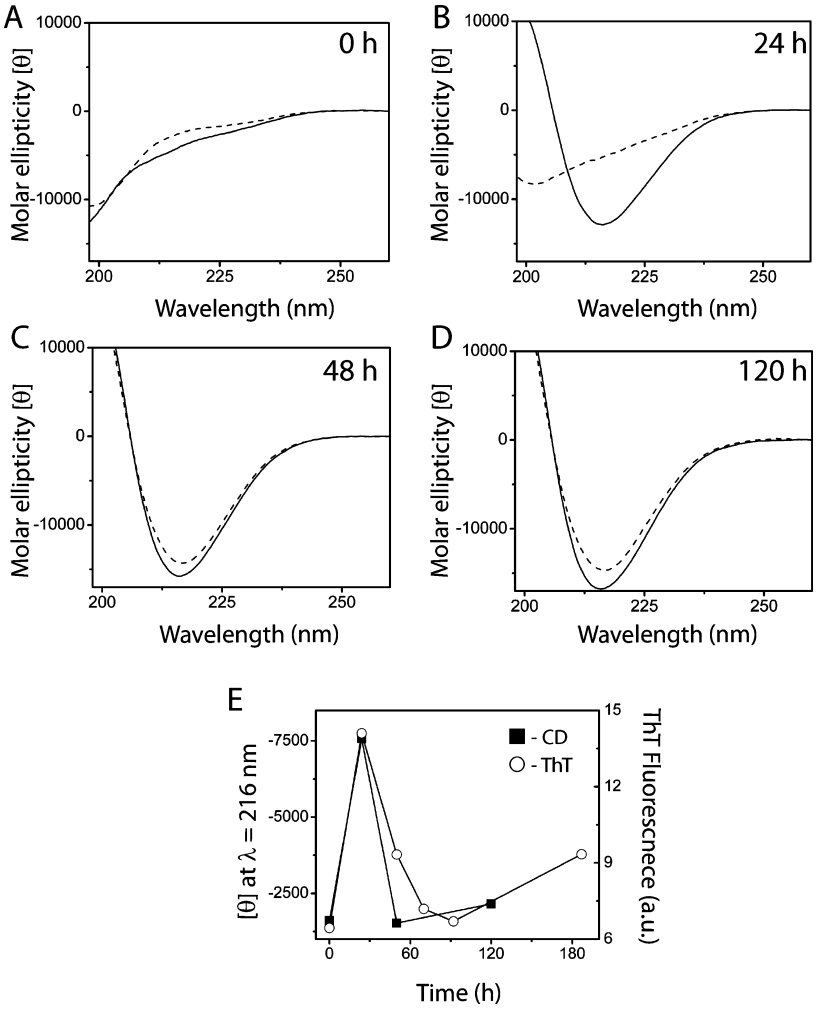

Figure 5. Secondary structure changes in Aβ42 upon incubation with BA. Coincubation reactions containing 4-fold molar excess of BA in EtOH similar to those shown in Figure 2C were monitored using far-UV CD (solid lines) along with a control in the absence of BA (dashed lines) at the indicated time points (A–D). (E) Difference plot obtained by subtracting the molar ellipticity values at 216 nm of the control sample from the sample containing BA (■), which was overlaid with the difference plot shown in Figure 2F for 1:4 stoichiometry (○).

aggregates. These results confirm that BA is able to promote insoluble fibril formation from Aβ42 monomer within 24 h and also suggest that this occurs in a manner that reduces the concentration of soluble, prefibrillar aggregates in the solution.

BA Induces Rapid Changes in Aβ42 Secondary Structure. The secondary structure changes during the incubation of Aβ42 with BA were monitored by far-UV CD spectroscopy. Since DMSO solvent is not compatible with CD measurements, Aβ42 was incubated with 4-fold excess of BA in 5% EtOH along with an appropriate control as in Figure 2C and D. Both the control sample and the one coincubated with BA displayed a random coil conformation immediately (10 min) after incubation (Figure 5A). However, the molar ellipticity at 216 nm was slightly more negative for the sample with BA, suggesting an immediate conformational change toward β-sheet. After 24 h of incubation, the sample containing BA clearly displayed a spectrum with negative minimum at 216 nm and positive maximum at ~198 nm, indicating a β-sheet conformation characteristic of Aβ fibrils (Figure 5B). In contrast, the control sample displayed predominantly a random coil structure (Figure 5B). After 48 h, both the control as well as the sample containing BA showed β-sheet conformation and remained in the same conformation for more than 120 h (Figure 5C and D). A comparison of the difference spectra obtained from ThT and CD experiments indicated identical changes (Figure 5E). It is clear that the maximal effect of BA was observed during the initial 24 h of incubation, which complements the results obtained from ThT, turbidity and sedimentation assays, along with immunoblots.

BA Binds to Monomeric Aβ42 with Sub-micromolar Binding Affinity. Finally, the binding interactions between Aβ42 and BA were explored by fluorescence anisotropy (FA). In order to do so, an F19W-Aβ42 mutant peptide was used in which the phenylalanine at the 19th position was substituted with a tryptophan residue to facilitate FA measurements. Although the wild-type Aβ contains a tyrosine (Tyr) residue at the 10th position, Tyr is not a good fluorophore and the emission intensities are prohibitively low for anisotropy experiments. F19W-Aβ40 mutant has been previously observed to exhibit no significant difference in aggregation and fibril formation compared to wild type Aβ40,[26] and hence, we anticipated similar behavior with Aβ42 also. To ensure that there was no significant difference between wild-type Aβ42 and the mutant, ThT experiments were performed both in the presence and in the absence of BA (Figure S1, Supporting Information). These experiments did not show significant

dx.doi.org/10.1021/cn300030a | ACS Chem. Neurosci. 2012, 3, 900–908

divergence from the aggregation profile of wild-type Aβ42. Upon titrating BA to a freshly purified monomeric F19W-Aβ42 sample, we observed a constant increase in tryptophan anisotropy (r) reflecting binding interaction between the two species (Figure 6; ●). Fitting the data using the noninteracting

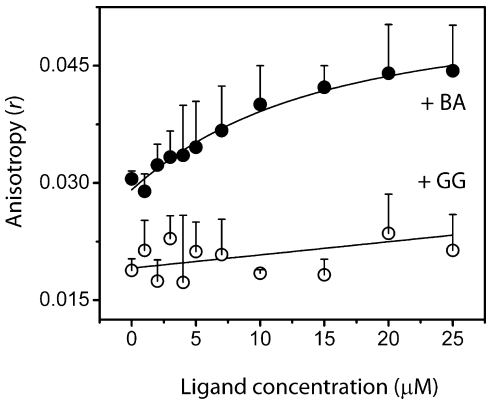

Figure 6. Binding affinity between Aβ42 and BA measured by fluorescence anisotropy. The specific mutant F19W-Aβ42 was used as a probe to measure tryptophan anisotropy (r). Aliquots of mixtures containing 5 μM Aβ42 and 50 μM BA in 2.5% DMSO were titrated on a solution containing 5 μM Aβ42 in a similar solvent (●). The anisotropy was measured in quadruplets and averaged for each titration point. As a negative control, a similar experiment was performed using glycyl-glycine instead of BA (○). Three independent data sets were averaged and fit with a model for single site binding (eq 2).

one-site binding equation (eq 2; Methods) yielded an apparent dissociation constant (K_D^{app} = 11.02 ± 2.01 μM). Since BA induces rapid aggregation especially at high molar ratios, the FA experiments may not reflect the binding interactions between BA and monomeric Aβ exclusively. For this reason, we refer to the binding affinity as "apparent", K_D^{app}. A dipeptide, glycyl-glycine (GG), was used as a negative control and did not show any appreciable binding isotherm (Figure 6; ○).

BA Specifically Affects Aggregates along the Fibril-Formation, "On-Pathway". It is becoming increasingly evident that Aβ can adopt alternative pathways of aggregation,[5−7] and that neurotoxic oligomers can also be populated via pathways other than the obligatory fibril-formation one.[9,10,27] For example, a 12−16mer oligomeric species of Aβ42 called "globulomers" was reported to be formed independently of the fibril formation pathway,[28] and a similar observation was reported for a 9−15mer species generated in the presence of SDS.[29] Recently, we reported the generation and isolation of a Aβ42 12−18mer species from fatty acids called large fatty acid-derived oligomers (LFAOs).[30] In the same report, we showed that LFAOs are "off-pathway" species and failed to convert to fibrils for an extended period of time. Therefore, we used LFAOs to explore whether BA is able to both affect their formation or promote fibril formation of isolated LFAOs (Figure 7). Clearly, BA failed to induce the formation of fibrils and concomitantly inhibit the formation of LFAOs under the conditions in which LFAOs are generated (Figure 7; lanes 1 and 2). In addition, BA failed to convert isolated LFAOs to fibrils rapidly as observed with monomers (Figure 7), suggesting that BA is unable to interact with oligomers that are not formed along the fibril formation, "on-pathway". In other words, the data suggests that BA specifically

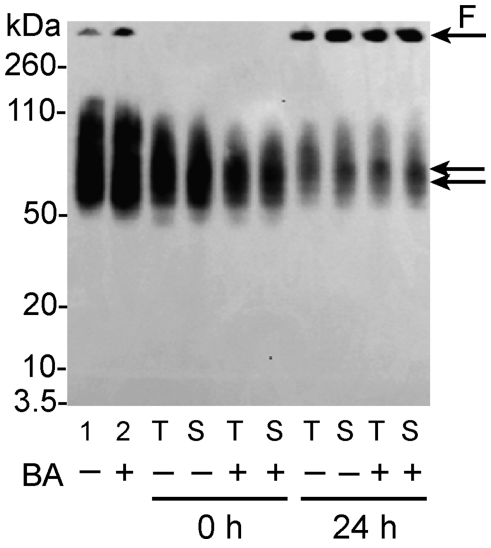

Figure 7. Effect of BA on "off-pathway" oligomers. Lanes 1 and 2 show 25 μM Aβ42 containing 5% DMSO incubated with 5 mM lauric acid alone and in the presence of 100 μM BA, respectively. In parallel, the SEC isolated oligomers were also incubated alone and with 100 μM BA at 37 °C. Aliquots of the sample were taken at the indicated time points and were electrophoresed and immunoblotted. Lanes T and S represent total and supernatant (after spinning the sample at 19,000g for 15 min to remove fibrils), respectively, after 0 and 24 h. The double arrows indicate LFAOs of Aβ42.

interacts with the "on-pathway" of aggregation toward fibril formation.

■ DISCUSSION

The rational design of Aβ aggregation inhibitors poses several challenges including; that (a) the difficulty in controlling the stage of inhibition during the aggregation process, and (b) the possible increase in the soluble oligomer concentrations upon inhibition of fibril formation may be detrimental, as smaller soluble oligomers are known to be more toxic than fibrils. Therefore, an ideal way of developing therapeutically viable aggregation inhibitors would be to trap Aβ at the monomeric level, since monomers are not toxic. However, it is difficult to design molecules against intrinsically disordered, monomeric Aβ due to its high conformational flexibility and lack of structurally well-defined recognition motifs. Considering such difficulties, it is not surprising that only a few aggregation inhibitors have successfully made it through clinical trials.

In this context, it is perhaps worthwhile to consider designing molecules that can prevent the formation of neurotoxic oligomers by circumventing these pathogenic species or by increasing their turnover rates. The results reported here suggest that BA is precisely able to perform such a task and showcase the potential use of BA as a therapeutic agent against AD. The mechanism of augmentation of aggregation by BA is not entirely a new observation as previously, compounds such as methylene blue and ellagic acid have also been reported to promote rapid Aβ42 fibril formation and inhibit neurotoxicity.[25,31] However, the rapid fibrillation induced by BA as reported here, which comes at the expense of toxic soluble oligomers, seems to be exclusive to the fibril formation "on-pathway". The data presented in this report suggest that (a) BA is extremely potent in promoting rapid fibril formation along the "on-pathway", and (b) BA is incapable of interacting with

dx.doi.org/10.1021/cn300030a | ACS Chem. Neurosci. 2012, 3, 900−908

aggregates along alternate pathways of aggregation. Although fibrils are not as toxic as the other soluble forms of Aβ aggregates such as oligomers, they can still cause cellular damage. However, by lowering the concentration of soluble oligomers as we have seen with BA, one could potentially lower the degree of toxicity and consequently slow down the progression of AD. In these respects, BA has considerable potential for use as a therapeutic agent for AD.

Pharmacologically, the properties of BA are well-known, and the compound is being administered for a variety of pathologies. Historically, extracts of *Bracopa monniera* have been used in Ayurvedic medicines for the treatment of CNS disorders and impaired mental function.[22,32] They are also thought to improve higher order cognitive processes that are critically dependent on the input of information from our environment such as learning and memory.[32] In addition, white birch bark, *Betula alba*, which contains BA, has been extensively used by native Americans to treat intestinal disorders. BA is also widely used in modern medicine.[23,33−37] BA has shown great promise as a potential therapeutic agent for a variety of cancer types, including neuroectodermal tumors, and is currently in phase II clinical trials for the treatment of dysplastic nevi with moderate to severe dysplasia. Furthermore, BA is also known to inhibit HIV viral replication.[38] Due to the distinct pharmacological advantages of BA as a therapeutic agent along with its unique property of promoting Aβ fibril formation and especially bypassing, or accelerating the clearance of toxic oligomers along the "on-pathway" fibril formation as reported here, BA can be a potential therapeutic candidate for AD. Therefore, understanding the effects of BA in *in vivo* systems such as cell culture and animal models is imperative for drug development. Our future experiments are focused on addressing these aspects and will be published at a later date.

METHODS

Materials. Aβ42 was synthesized at the Peptide Synthesis Facility at the Mayo Clinic (Rochester, MN) using routine Fmoc chemistry. MALDI-TOF mass spectrometry revealed >90% purity of both peptides. BA, SDS, bovine serum albumin, and thioflavin-T were procured from Sigma Aldrich Inc. (St. Louis, MO). All other chemicals were obtained from VWR Inc.

Preparation of Aβ42 Monomers. Lyophilized stocks of synthetic Aβ42 were stored at −20 °C, desiccated. Prior to the experiments, any preformed aggregates that may have been present were removed via size exclusion chromatography (SEC) as previously reported.[30] Briefly, 1−1.5 mg of the peptide was dissolved in 0.5 mL of 30 mM NaOH, and allowed to stand at room temperature for 15 min before loading onto a Superdex-75 HR 10/30 size exclusion column (SEC) (GE Life Sciences) attached to an AKTA FPLC system (GE Healthcare, Buckinghamshire). The column was pre-equilibrated in 20 mM Tris-HCl (pH 8.0) at 25 °C and was run at a flow rate of 0.5 mL/min. One minute fractions were collected. Concentrations of the purified fractions were estimated by UV−vis spectroscopy on a Cary 50 spectrophotometer (Varian Inc.) using a molar extinction coefficient (ε) of 1490 cm^{-1} M^{-1} (www.expasy.org), corresponding to the single tyrosine residue within Aβ42. Peptide integrity after SEC was again confirmed by MALDI-TOF mass spectrometry, which yielded a single peak corresponding to a monoisotopic molecular mass of 4516.31 Da in a good agreement with the calculated mass of 4514.13 Da. A similar purification scheme was also adopted for mutant F19W-Aβ42. Monomeric Aβ42 fractions were stored at 4 °C and were used within a day of purification in all experiments to avoid the presence of preformed aggregates in our reactions as previously reported.[29] Monomer samples more than a day old were tested for aggregation by ThT fluorescence prior to their use.

Aβ42 Oligomer Generation. Aβ42 12−18mers (LFAOs) were generated by following the method reported previously.[30] Briefly, 50 μM Aβ42 was incubated with 5 mM lauric acid at 37 °C for 48 h. The sample was then fractionated using a Superdex-75 SEC column, and the fractions 17 and 18 were collected for further use.

Aβ Aggregation Reactions. Unless otherwise noted, all reactions were incubated at 37 °C while the measurements were done at room temperature by taking aliquots of the incubated samples. Reactions were initiated in 0.5 mL siliconized Eppendorf tubes by incubating the freshly purified Aβ42 monomer in appropriate conditions in buffer without agitation. Aggregation parameters were obtained by monitoring the reaction with thioflavin T (ThT) fluorescence and fitting fluorescence data points to the sigmoidal curve in eq 1 using Origin 7.0.

$$F = \frac{a}{1 + e^{-[(t - t_{0.5})/b]}} \quad (1)$$

In this equation, t is time, a and b are fixed parameters, and $t_{0.5}$ is the time to reach half-maximal ThT fluorescence. Lag times were equal to $t_{0.5} - 2b$ for each fitted curve.

Fluorescence Spectroscopy. *ThT Fluorescence.* Fluorescence (F) was monitored in a 1 cm quartz microcuvette on a Cary Eclipse spectrometer (Varian Inc.) after 15-fold dilution of Aβ42 samples into 5 mM Tris-HCl (pH 8.0) containing 10 μM ThT. Continuous measurements of F were taken for 1 min with the excitation and emission wavelengths fixed at 450 and 482 nm respectively, and a bandwidth of 20 nm (10/10). The fluorescence blanks were subtracted from the respective data and the average F value was determined. For kinetics experiments, Aβ samples immediately after incubation were similarly diluted into 10 μM ThT buffer, and continuous fluorescence measurements were measured for 15 min with 10s data interval but with same other parameters as above.

Anisotropy. Binding experiments were carried out via fluorescence anisotropy by monitoring the tryptophan residue on a F19W-Aβ42 mutant. The excitation and emission wavelengths were fixed at 280 and 352 nm, respectively, with a spectral bandwidth of 30 nm (10 nm Ex and 20 nm Em).

$$r = r_0 - \left[\frac{(r_0 - r_s)}{2P_t}\right]\left[(K_d + L_t + P_t) - \sqrt{(K_d + L_t + P_t)^2 - 4L_tP_t}\right] \quad (2)$$

The ADL program provided by the manufacturer was used and the G-factor was calculated for each titration using F19W-Aβ42 as the fluorophore. Each titration point was measured in quadruplets after a brief equilibration time of 1 min, and the data points were averaged. The data was converted to anisotropy (r) values using the "Advanced Read" program provided by the manufacturer. The data were fit to a noncooperative single site binding equation using Origin 7.0 (eq 2), where r_0 and r_s are anisotropy values in the absence and saturated levels of the ligand (BA), respectively, while L_t and P_t are the respective total ligand and Aβ42 concentrations.

Turbidity Assay. Turbidity was monitored in a 1 cm quartz microcuvette using a Cary 50 UV−vis spectrophotometer (Agilent Technologies). At the given time points, a 70 μL aliquot of the Aβ aggregation reaction was placed into the cuvette and absorbance was measured at 400 nm using the "Simple Read" program provided by the manufacturer in triplicates with 30 s delays. For kinetics experiments, Aβ samples immediately after incubation were monitored without dilution at the same wavelength using the "Kinetics" program from the manufacturer.

Size Exclusion Chromatography (SEC). Quantitative estimates of aggregation reaction were obtained using a Superdex-75 HR 10/30 size exclusion column (GE Life Sciences) on an AKTA FPLC system. Aliquots of sample from the aggregation reactions were centrifuged, and the supernatant (100 μL) was loaded onto the SEC column. The samples were then subjected to fractionation in 20 mM Tris-HCl, pH 8.0 at a constant flow rate of 0.5 mL/min, and the elution was monitored at the wavelength of 215 nm.

Polyacrylamide Gel Electrophoreses (PAGE) and Immunoblotting. Samples were dissolved in loading buffer (1× Laemmli buffer) containing 1% SDS, applied without heating to 4−12% NuPage gels (Invitrogen) containing bis-Tris, and resolved in 2-(*N*-morpholino)ethanesulfonic acid (MES) running buffer with 0.1% SDS. Dye-linked MW markers (Blue Plus2 Prestained Standards, Invitrogen) were run in parallel for calibration. Gels were electroblotted onto 0.45 μm immobilon nitrocellulose membranes (BioTrace NT, Life Sciences Inc.). Blots were boiled in a microwave oven in PBS for 2 min and were blocked overnight with 1× PBS containing 5% nonfat dry milk and 0.1% Tween-20 before probing (1−2 h) with 1:1000−1:2500 dilutions of Ab9 monoclonal antibody, which detects amino acid residues of Aβ (1−16). Blots were then incubated with anti-mouse horseradish peroxide (HRP) conjugate and developed with ECL reagent (Thermo Scientific).

Circular Dichroism (CD). Far-UV CD spectra were obtained with a Jasco J-815 spectropolarimeter (Jasco Inc., Easton, MD). Aliquots of samples containing Aβ42 (25 μM) were placed in a 0.1 cm path length quartz cuvette (Hellma) and were monitored in continuous scan mode (260−190 nm). The acquisition parameters were 50 nm/min with 8 s response time, 1 nm bandwidth, and 0.1 nm data pitch, and data sets were averaged over three scans. All data were collected in duplicate. Spectra of appropriate blanks were subtracted from the data sets as indicated. The corrected, averaged spectra were smoothed using the "means-movement" algorithm with a convolution width of 25 using the Jasco spectra analysis program.

■ ASSOCIATED CONTENT

Ⓢ Supporting Information

Additional figure showing aggregation of F19W-Aβ42 as measured via ThT fluorescence over time. This material is available free of charge via the Internet at http://pubs.acs.org.

■ AUTHOR INFORMATION

Corresponding Author

*E-mail: vijay.rangachari@usm.edu. Telephone: (601) 266-6044. Fax: (601) 266-6075.

Author Contributions

V.R. conceived and designed the project, and M.S.P., M.A.S., and A.K. were involved in conducting experiments such as fluorescence, SEC, CD, and immunoblotting. M.S.P. also assisted in the preparation of the manuscript with V.R.

Funding

The authors thank the American Heart Association (10GRNT4190124) for their financial support (for V.R.). This work was also supported by the Mississippi INBRE funded by grants from the National Center for Research Resources (5P20RR016476-11) and the National Institute of General Medical Sciences (8 P20 GM103476-11) from the National Institutes of Health.

Notes

The authors declare no competing financial interest.

■ ABBREVIATIONS

SEC, size exclusion chromatography; Aβ, amyloid-β; CD, circular dichroism; DMSO, dimethyl sufoxide; BA, betullinic acid; MALDI-ToF, matrix-assisted laser desorption ionization; FA, fluorescence anisotropy; PBS, phosphate buffer saline; EtOH, ethanol

■ REFERENCES

(1) Hartley, D. M., Walsh, D. M., Ye, C. P., Diehl, T., Vasquez, S., Vassilev, P. M., Teplow, D. B., and Selkoe, D. J. (1999) Protofibrillar intermediates of amyloid beta-protein induce acute electrophysiological changes and progressive neurotoxicity in cortical neurons. *J. Neurosci. 19*, 8876−8884.

(2) Kawarabayashi, T., Shoji, M., Younkin, L. H., Wen-Lang, L., Dickson, D. W., Murakami, T., Matsubara, E., Abe, K., Ashe, K. H., and Younkin, S. G. (2004) Dimeric amyloid beta protein rapidly accumulates in lipid rafts followed by apolipoprotein E and phosphorylated tau accumulation in the Tg2576 mouse model of Alzheimer's disease. *J. Neurosci. 24*, 3801−3809.

(3) Lesne, S., Koh, M. T., Kotilinek, L., Kayed, R., Glabe, C. G., Yang, A., Gallagher, M., and Ashe, K. H. (2006) A specific amyloid-beta protein assembly in the brain impairs memory. *Nature 440*, 352−357.

(4) Shankar, G. M., Li, S., Mehta, T. H., Garcia-Munoz, A., Shepardson, N. E., Smith, I., Brett, F. M., Farrell, M. A., Rowan, M. J., Lemere, C. A., Regan, C. M., Walsh, D. M., Sabatini, B. L., and Selkoe, D. J. (2008) Amyloid-beta protein dimers isolated directly from Alzheimer's brains impair synaptic plasticity and memory. *Nat. Med. 14*, 837−842.

(5) Goldsbury, C., Frey, P., Olivieri, V., Aebi, U., and Muller, S. A. (2005) Multiple assembly pathways underlie amyloid-beta fibril polymorphisms. *J. Mol. Biol. 352*, 282−298.

(6) Gorman, P. M., Yip, C. M., Fraser, P. E., and Chakrabartty, A. (2003) Alternate aggregation pathways of the Alzheimer beta-amyloid peptide: Abeta association kinetics at endosomal pH. *J. Mol. Biol. 325*, 743−757.

(7) Jahn, T. R., and Radford, S. E. (2007) Folding versus aggregation: Polypeptide conformations on competing pathways. *Arch. Biochem. Biophys.*,.

(8) Bitan, G., Fradinger, E. A., Spring, S. M., and Teplow, D. B. (2005) Neurotoxic protein oligomers--what you see is not always what you get. *Amyloid 12*, 88−95.

(9) Huang, T. H., Yang, D. S., Fraser, P. E., and Chakrabartty, A. (2000) Alternate aggregation pathways of the Alzheimer beta-amyloid peptide. An in vitro model of preamyloid. *J. Biol. Chem. 275*, 36436−36440.

(10) Lambert, M. P., Barlow, A. K., Chromy, B. A., Edwards, C., Freed, R., Liosatos, M., Morgan, T. E., Rozovsky, I., Trommer, B., Viola, K. L., Wals, P., Zhang, C., Finch, C. E., Krafft, G. A., and Klein, W. L. (1998) Diffusible, nonfibrillar ligands derived from Abeta1−42 are potent central nervous system neurotoxins. *Proc. Natl. Acad. Sci. U.S.A. 95*, 6448−6453.

(11) Tjernberg, L. O., Naslund, J., Lindqvist, F., Johansson, J., Karlstrom, A. R., Thyberg, J., Terenius, L., and Nordstedt, C. (1996) Arrest of beta-amyloid fibril formation by a pentapeptide ligand. *J. Biol. Chem. 271*, 8545−8548.

(12) Bohrmann, B., Adrian, M., Dubochet, J., Kuner, P., Muller, F., Huber, W., Nordstedt, C., and Dobeli, H. (2000) Self-assembly of beta-amyloid 42 is retarded by small molecular ligands at the stage of structural intermediates. *J. Struct. Biol. 130*, 232−246.

(13) Ono, M., Kung, M. P., Hou, C., and Kung, H. F. (2002) Benzofuran derivatives as Abeta-aggregate-specific imaging agents for Alzheimer's disease. *Nucl. Med. Biol. 29*, 633−642.

(14) Ono, K., Hasegawa, K., Yoshiike, Y., Takashima, A., Yamada, M., and Naiki, H. (2002) Nordihydroguaiaretic acid potently breaks down pre-formed Alzheimer's beta-amyloid fibrils in vitro. *J. Neurochem. 81*, 434−440.

(15) Pallitto, M. M., Ghanta, J., Heinzelman, P., Kiessling, L. L., and Murphy, R. M. (1999) Recognition sequence design for peptidyl modulators of beta-amyloid aggregation and toxicity. *Biochemistry 38*, 3570−3578.

(16) Giri, R. K., Rajagopal, V., and Kalra, V. K. (2004) Curcumin, the active constituent of turmeric, inhibits amyloid peptide-induced cytochemokine gene expression and CCR5-mediated chemotaxis of THP-1 monocytes by modulating early growth response-1 transcription factor. *J. Neurochem. 91*, 1199−1210.

(17) Yang, F., Lim, G. P., Begum, A. N., Ubeda, O. J., Simmons, M. R., Ambegaokar, S. S., Chen, P. P., Kayed, R., Glabe, C. G., Frautschy, S. A., and Cole, G. M. (2005) Curcumin inhibits formation of amyloid beta oligomers and fibrils, binds plaques, and reduces amyloid in vivo. *J. Biol. Chem. 280*, 5892−5901.

(18) Sato, T., Kienlen-Campard, P., Ahmed, M., Liu, W., Li, H., Elliott, J. I., Aimoto, S., Constantinescu, S. N., Octave, J. N., and Smith, S. O. (2006) Inhibitors of amyloid toxicity based on beta-sheet packing of Abeta40 and Abeta42. *Biochemistry 45*, 5503−5516.
(19) Kokkoni, N., Stott, K., Amijee, H., Mason, J. M., and Doig, A. J. (2006) N-Methylated Peptide Inhibitors of beta-Amyloid Aggregation and Toxicity. Optimization of the Inhibitor Structure. *Biochemistry 45*, 9906−9918.
(20) Rangachari, V, D., Z., Healy, B, Moore, B. D., Sonoda, L. K., Cusack, B, Maharvi, G. M., Fauq, A. H., and Rosenberry, T. L. (2009) Rationally designed dehydroalanine (DAla) containing peptides inhibit amyloid-beta(Ab) peptide aggregation. *Biopolymers 91*, 456−465.
(21) Yogeeswari, P., and Sriram, D. (2005) Betulinic acid and its derivatives: a review on their biological properties. *Curr. Med. Chem. 12*, 657−666.
(22) Bhattacharya, S. K., Bhattacharya, A., Kumar, A., and Ghosal, S. (2000) Antioxidant activity of Bacopa monniera in rat frontal cortex, striatum and hippocampus. *Phytother. Res. 14*, 174−179.
(23) Fulda, S., Friesen, C., Los, M., Scaffidi, C., Mier, W., Benedict, M., Nuez, G., Krammer, P., Peter, M., and Debatin, K.-M. (1997) Betulinic Acid Triggers CD95 (APO-1/Fas)- and p53-independent Apoptosis via Activation of Caspases in Neuroectodermal Tumors. *Cancer Res. 57*, 4956−4964.
(24) LeVine, H., 3rd. (1993) Thioflavine T interaction with synthetic Alzheimer's disease beta-amyloid peptides: detection of amyloid aggregation in solution. *Protein Sci. 2*, 404−410.
(25) Necula, M., Breydo, L., Milton, S., Kayed, R., van der Veer, W. E., Tone, P., and Glabe, C. G. (2007) Methylene blue inhibits amyloid Abeta oligomerization by promoting fibrillization. *Biochemistry 46*, 8850−8860.
(26) Touchette, J. C., Williams, L. L., Ajit, D., Gallazzi, F., and Nichols, M. R. (2009) Probing the amyloid-beta(1−40) fibril environment with substituted tryptophan residues. *Arch. Biochem. Biophys. 494*, 192−197.
(27) Bitan, G., Lomakin, A., and Teplow, D. B. (2001) Amyloid beta-protein oligomerization: prenucleation interactions revealed by photo-induced cross-linking of unmodified proteins. *J. Biol. Chem. 276*, 35176−35184.
(28) Gellermann, G. P., Byrnes, H., Striebinger, A., Ullrich, K., Mueller, R., Hillen, H., and Barghorn, S. (2008) Abeta-globulomers are formed independently of the fibril pathway. *Neurobiol. Dis. 30*, 212−220.
(29) Rangachari, V., Moore, B. D., Reed, D. K., Bridges, A. W., Conboy, E., Hartigan, D., and Rosenberry, T. L. (2007) Amyloid-β(1−42) Rapidly Forms Protofibrils and Oligomers by Distinct Pathways in Low Concentrations of Sodium Dodecylsulfate. *Biochemistry 46*, 12451−12462.
(30) Kumar, A., Rice, B. L., Patel, P., Paslay, L. C., Singh, D., Bienkiewicz, E. A., Morgan, S. E., and Rangachari, V. (2011) Non-esterified Fatty Acids Generate Distinct Low-molecular Weight Amyloid-b (Ab42) Oligomers along pathway Different from Fibril Formation. *PLoS One 6*, e18759.
(31) Feng, Y., Yang, S. G., Du, X. T., Zhang, X., Sun, X. X., Zhao, M., Sun, G. Y., and Liu, R. T. (2009) Ellagic acid promotes Abeta42 fibrillization and inhibits Abeta42-induced neurotoxicity. *Biochem. Biophys. Res. Commun. 390*, 1250−1254.
(32) Stough, C, L., J., Clarke, J, Downey, L. A., Hutchison, C. W., Rodgers, T, and Nathan, P. J. (2001) The chronic effects of an extract of Bacopa monniera (Brahmi) on cognitive function in healthy human subjects. *Psychopharmacology (Berlin, Ger.) 156*, 481−484.
(33) Mukherjee, R., Jaggi, M., Rajendran, P., Siddiqui, M., Srivastava, S., Vardhan, A., and Burman, A. (2004) Betulinic acid and its derivatives as anti-angiogenic agents. *Bioorg. Med. Chem. Lett. 14*, 2181−2184.
(34) Fujioka, T., Kashiwada, Y., Kilkuskie, R., Cosentino, M., Ballas, L., Jiang, J., Janzen, W., Chen, I.-S., and Lee, K.-H. (1994) Anti-AIDS Agents, 11. Betulinic Acid and Platanic Acid as Anti-HIV Principles from Syzigium claviflorum, and the Anti-HIV Activity of Structurally Related Triterpenoids. *J. Nat. Prod. 57*, 243−247.
(35) Pisha, E., Chai, H., Lee, I.-S., Chagwedera, T., Farnsworth, N., Cordell, G., Beecher, C., Fong, H., Kinghorn, D., Brown, D., Wani, M., Wall, M., Hieken, T., Das Gupta, T., and Pezzuto, J. (1995) Discovery of betulinic acid as a selective inhibitor of human melanoma that functions by induction of apoptosis. *Nat. Med. 1*, 1046−1051.
(36) Eiznhamer, D. A., and Xu, Z. Q. (2004) Betulinic acid: A promising anticancer candidate. *IDrugs 7*, 359−373.
(37) Zuco, V., Supino, R., Righetti, S., Cleris, L., Marchesi, E., Gambacorti-Passerini, C., and Formelli, F. (2002) Selective cytotoxicity of betulinic acid on tumor cell lines, but not on normal cells. *Cancer Lett. 175*, 17−25.
(38) Kashiwada, Y., Hashimoto, F., Cosentino, L. M., Chen, C.-H., Garrett, P. E., and Lee, K.-H. (1996) Betulinic Acid and Dihydrobetulinic Acid Derivatives as Potent Anti-HIV Agents1. *J. Med. Chem. 39*, 1016−1017.